

METAL-INSULATOR-METAL (MIM) NANOCAPACITORS AND EFFECTS OF MATERIAL PROPERTIES ON THEIR OPERATION

S. R. Ekanayake^{1,2}, M. Ford² and M. Cortie²

¹ Faculty of Engineering, ² Institute for Nanoscale Technology,
University of Technology, Sydney, PO Box 123, Broadway, NSW, 2007, Australia

ABSTRACT

Metal-insulator-metal (MIM) capacitors play an important part in many integrated electronic circuits in the areas of analog, microwave, and radio frequency systems. However the transverse dimensions of current MIM capacitors are in the micrometer scale. If integrated circuits continue to be miniaturized, the capacitor, alongside other components, must also be miniaturized to realize nanoelectronic circuits and systems. This article presents a novel device, the nanocapacitor, of which the dimensions are constrained to nanoscale in longitudinal and transverse directions, and discusses the effects of material properties on their operation. In particular, this work discusses the effects of dielectric constant, dielectric strength, and quantum electrical phenomena on achieving relatively high capacitances and capacitance densities in nanocapacitors.

Keywords: Capacitors, Dielectric thin films, Nanoelectronic devices, Single electron devices

1. INTRODUCTION

The resolution of feature sizes in integrated circuits (ICs) has been reducing linearly as predicted by the ITRS¹, and is rapidly approaching nanoscale. This rapid reduction has lead to an explosion in nanoscale exploration to improve conventional devices, and develop novel devices that utilize quantum-size phenomena inherent at this scale.

Increasing IC densities have many benefits including lower current propagation times, higher clock frequencies, larger circuit real estate, and higher integration. While immersing nanoelectronic technologies encourage nanoscale IC (nanocircuit) design, currently, their emphasis is on the nanoscale transistor. However, if nanocircuits are expected to be viable, components other than the transistor must also be developed at the nanoscale. The capacitor is one of the four fundamental circuit elements required to design a feasible nanocircuit, and is a critical component in electronic circuits.^{2,3} Hence the capacitor, amongst other components, must also be developed at nanoscale towards prototyping functional nanocircuits.

The nanocapacitor presented in this work, is a metal-insulator-metal (MIM) device with all spatial dimensions constrained to nanoscale.⁴ Hence it is affected by physicochemical properties of the materials from which it is fabricated, and quantum-size phenomena. Additionally, they overcome one of the limitations of current integrated capacitor design, which is their requirement of large physical size for usable capacitances, relative to other components on-die.^{3,5}

There has been some recent work investigating the behavior of nanocapacitors. Maccuci^{6,7} presented

modeling of differential capacitance of radial quantum dots, and Wang *et al.* presented work on non-linear quantum capacitance⁸ and capacitance of atomic junctions.⁹ This work presents the material properties that may influence the feasibility and operation of nanocapacitors, and proposes the nanocapacitor as a device that could have applications in low power nanoelectronic circuits such as biochemically^{10,11} and microbattery¹² powered circuits, hybrid (microelectronic-nanoelectronic) systems, and low charge store-pump applications. A radial parallel plate (RPP) setup is used such as that illustrated in Figure 1 for simplicity, to present the materials dependent effects on nanocapacitor structures, which can be developed using various atomic layer deposition techniques as well as recently developed nanolithography techniques.^{13,14}

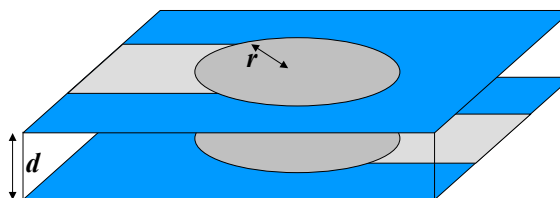


Figure 1. Radial parallel-plate (RPP) nanocapacitor, as may be fabricated using modern nanolithographic techniques, and molecular vapor deposition. The surface (blue) encompasses the dielectric slab of thickness d , and the cylinders on the top and bottom of the dielectric slab are the metal electrodes of radius r contacted by the leads (tracks), whose area determines the capacitive volume.

Section 2 presents the design of RPP nanocapacitors and inherent material properties that may affect their

feasibility and operation. Section 3 presents quantum electrical characteristics that could affect the capacitance, and capacitance density due to the electronic properties of the contacts of the nanocapacitor, and concludes with some applications.

2. DESIGN OF NANOCAPACITORS

The conceptual RPP capacitors used in this work have two disk electrodes separated by a radial thin-film dielectric of which the electrostatic capacitance is

$$C = \epsilon_r \epsilon_0 A / d \quad (1)$$

and the electrical potential energy stored is

$$U_e = \frac{1}{2} C \phi^2 \quad (2)$$

where ϵ_r is the dielectric constant, and ϵ_0 (F/m) is the absolute permittivity, d (m) is the longitudinal dielectric thickness, A (m²) is the polarizable area of radius r (m), ϕ (V) is the applied potential difference, and U_e (J) the electric potential energy stored.

Electrostatic phenomena are considered scale invariant hence one can use expressions (1), and (2), correctly.¹⁵ However, at these dimensions, the quantized nature of charge, and stored electrical energy becomes apparent. Evaluating for the RPP model, using SiO₂ as the dielectric where $\epsilon_r(\text{SiO}_2) = 3.9$, and gold (Au) for the electrodes with plate radius, $r = 1$ nm, and dielectric thickness, $d = 0.5$ nm, which is attainable with modern growth techniques, a capacitance of 0.22 aF can be obtained. The potential difference produced across the capacitor due to the stored charge is given by

$$\phi = Q / C \quad (3)$$

and is 0.74 V for a single electron, where Q (C) is the total charge, stored. Therefore the stored electrical energy is 0.37 eV. The electric field produced within the dielectric is 15 MV/cm and is at the threshold of currently known dielectric strengths. Hence this is a single electron capacitor (SEC), which can be used in single-electron memory¹⁶ devices.

2.1 Dielectric constant

In the RPP nanocapacitor, the only parameter that can be adjusted to vary the capacitance is the dielectric constant, ϵ_r . Hence the dielectric's structure plays a significant part in nanocapacitor design as the tensor nature of the dielectric constant may become apparent at nanoscale. However, the dielectric constant is a bulk property, which requires a lattice for its validity. Despite the nanoscale dimensions of the contacts, and its polarizable element (the dielectric), the nanocapacitor in this work is composed of thousands of atoms in an arbitrary lattice depending on the materials used. Therefore in the context of this discussion, the scalar dielectric constant applicable to bulk materials is used.

Several solid-state insulators are considered as potential dielectrics for nanocapacitors. These are, *inter alia*, SiO₂, and Al₂O₃ mainly due to their high band gaps of 9

eV and 11 eV, respectively. The high band gaps of these dielectrics allow nanocapacitors to operate at high electric fields, and minimize charge leakage through thermionic emission, or tunneling. Other candidates include Ta₂O₅, TiO₂, and monolayers of organic or inorganic molecules.

The effect of the dielectric constant on the capacitance and capacitance density is evident from Figure 2, shown for some general dielectrics currently used for capacitors, and the candidates chosen for RPP nanocapacitor design. Note that, of the lower dielectric constants, the vacuum capacitance density is 9 fF/μm² for $d = 1$ nm, while of the higher dielectric constants, the TiO₂ capacitance density is 885 fF/μm². These capacitance densities are as high as, or greater than those of current integrated MIM capacitors, and contribute further towards the feasibility of these devices. The selection of SiO₂ for this discussion is based on its currently understood properties, and widely available literature, which provides an electrostatic capacitance density of 35 fF/μm² for $d = 1$ nm, in this design.

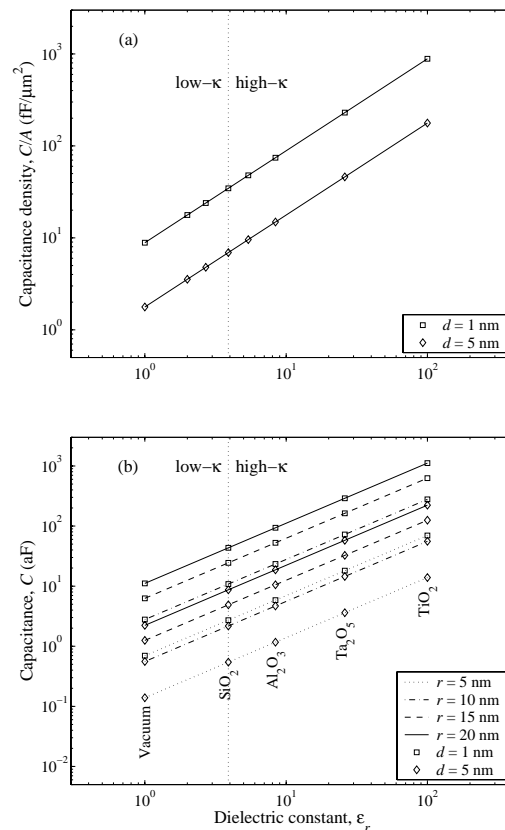


Figure 2. (a) Capacitance density, and (b) capacitance to dielectric constant for the dielectrics shown in (b) illustrating the effect of ϵ_r on the capacitance of the RPP nanocapacitor of contact radius r (nm), and dielectric thickness d (nm).

2.2 Dielectric strength

Silicon dioxide has desirable properties in bulk and at nanoscale. However, there is the possibility of defect generation through charge traps both in bulk and nanoscale thin-films as Bersuker *et al.* have shown.¹⁷ Hence, dielectric breakdown can occur through the above phenomenon of defect formation through trapped electrons in localized states within the dielectric's potential barrier. These localized states can occur due to localized quantum wells produced by impurity atoms within the potential barrier of the dielectric, non-terminated interfacial bonds leading to dangling bonds, and embedded structural defects within the bulk of the thin-film. These are illustrated in Figure 3.

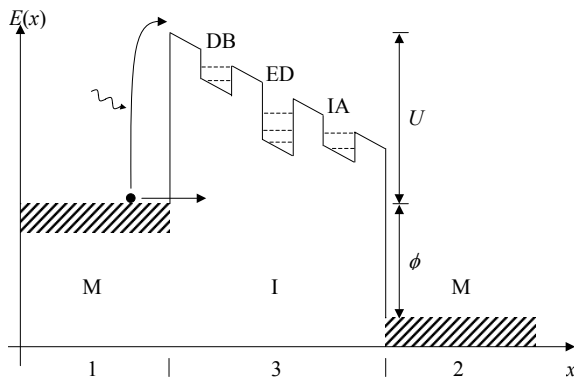


Figure 3. Potential function of a MIM nanocapacitor with dielectric defects such as impurity atoms (IAs), non-terminated bonds (dangling bonds) (DBs), and embedded defects (EDs) within its bulk. Quantized quasi-bound states produce resonances within quantum wells formed at the conduction band edge of the dielectric due to these defects, which will produce resonant tunneling which can result in enhanced charge loss in certain regions of the I-V characteristics of the nanocapacitor. Such behavior will have undesirable effects on the I-V, and C-V curves of the nanocapacitor. Hence it is necessary to produce defect free dielectrics during deposition of the materials for proper fabrication and operation of nanocapacitors.

This work does not tabulate dielectric strengths for any material, as this quantity is a dynamic function of the longitudinal thickness of the dielectric, and the frequency of the applied electric field.⁴ Hence the dielectric strength of a material will vary between samples. This may also be the reason, why much of the literature has no dielectric strengths quoted, apart from well-studied dielectrics such as SiO₂ at microscale or nanoscale.

2.3 Maximizing capacitance density

As circuit dimensions reduce to nanoscale so will the need for coupling and decoupling capacitance. Hence the capacitance of nanocapacitors can be sufficient. However if larger capacitances are required, it is beneficial to maximize their capacitance densities by

designing them to utilize transverse components of the electric field as well as its longitudinal component. There are two ways of increasing the capacitance density of nanocapacitors: using high- κ dielectrics, and increasing the surface area exposed to the electric field. However, in the former, one must ensure the dielectric's electrical stability, which depends on the purity and material properties of both the dielectric, and contact regions. In the latter, designing 3D structures such as coaxial, and clustered nanoparticle¹⁸ structures may be advantageous, as these allow reduced fringe effects and increased densities.

Aparacio *et al.*¹⁵ reported on developing microscopic fractal and interdigital configurations in an attempt to increase capacitance densities of their structures. Such structures may also be made at the nanoscale using nanoscopic solid-state dielectrics, or organic dielectrics such as self-assembled-monolayers¹⁹ (SAMs) in fractal or interdigital setups. Such fractal and interdigital setups may also be useful when increasing the capacitance density of nanocapacitors.

3. QUANTUM ELECTRICAL PHENOMENA

3.1 Reduced screening of quantum sized contacts

A correction to the purely electrostatic (classical) capacitance model for RPP capacitance is used, taking into account the effects of the low density of states (DOS) of the contacts assuming the leads and bulk of the electrodes are thermodynamic electron reservoirs governed by Fermi-Dirac statistics. The contact is the local interface region of the electrodes, and dielectric where the potential function usually changes abruptly. This correction takes into account the electrochemical (quantum) capacitance due to the Fermi-Dirac distribution of electrons in the nanoscale contacts. The low DOS of the contacts means lesser electron states available for occupation resulting in reduced screening. This allows the applied electric field to penetrate the surface of the contact by a distance known as the Thomas-Fermi screening length (radius). This length increases with decreasing DOS producing a surface-body charge gradient in the contact, which emulates the electrochemical capacitance. In fact, physically, the electrochemical capacitances are in series with the electrostatic capacitance such that the equivalent electrochemical capacitance can in general be written as $R/C = 1/C_s + \sum_i 1/C_{\mu i}$ where for this case $i = 1, 2$ for the two conductors. Figure 4 illustrates this capacitance model from which one can derive the correction as follows.

The equivalent electrochemical capacitance resulting from the series impedances of the electrostatic and electrochemical capacitances of the model in Figure 4b is

$$C = R \left(\frac{1}{C_s} + \frac{1}{C_{\mu 1}} + \frac{1}{C_{\mu 2}} \right)^{-1} \quad (4)$$

where C_s is the electrostatic capacitance, $C_{\mu 1}$ and $C_{\mu 2}$ are the electrochemical capacitances $e^2 \int_V (dN_1/dE) d^3 \mathbf{r}$ and $e^2 \int_V (dN_2/dE) d^3 \mathbf{r}$ due to the global total DOS dN_1/dE and dN_2/dE of the contacts 1 and 2, respectively, and $R = 1$ is the reflection coefficient set to simulate total scattering of incident electrons injected into the dielectric potential barrier. This is based on the assumption that the DOS of the contacts tends towards that of the bulk structures as it increases in size, thus the screening length tends towards zero as the electric field approaches the surface, causing the electrochemical capacitance components to vanish.

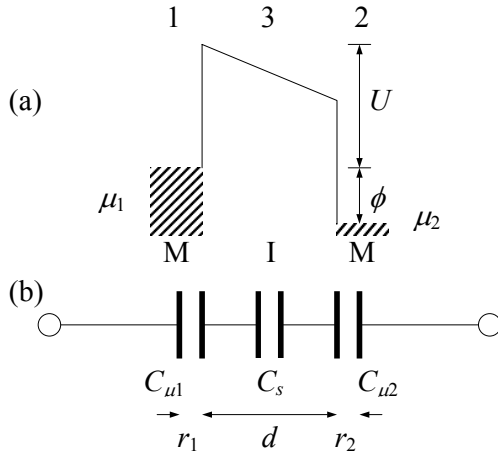


Figure 4. (a) The band diagram of a MIM nanocapacitor under applied bias ϕ , with metal regions 1 and 2, and dielectric region 3, and (b) the schematic of equivalent capacitance from the electrostatic and electrochemical capacitances of the RPP architecture, due to Thomas-Fermi screening lengths of the interfacial metal contacts.

If the electrodes are made of the same metal and are identical, the capacitance in (4) can be simplified using the Thomas-Fermi screening length of the metal contacts as

$$C = \left(\frac{2}{C_{\mu 1, \mu 2}} + \frac{d}{\epsilon_r \epsilon_0 A} \right)^{-1} \quad (5)$$

where the capacitances of the contacts due to the low DOS are²⁰

$$C_{\mu 1} = C_{\mu 2} = \frac{\epsilon_m \epsilon_0 A}{r_{TF} \sqrt{\epsilon_m}}, \quad (6)$$

given that the screening length is²¹

$$r_{TF} = r_{1,2} = \left(\frac{\epsilon_0}{e^2 D_{1,2}(\mu_F)} \right)^{1/2} = \frac{(r_s/a_0)^{1/2}}{2.95 \cdot 10^{10}} \quad (7)$$

The dielectric constant of metal electrodes $\epsilon_m = 5$, in this work. In (7), e is the elementary charge ($1.6022 \cdot 10^{-19}$ C), and $D_{1,2}(\mu_F) = dN_{1,2}/d\mu_{1,2}$ is the DOS at the electrochemical (Fermi) potential of either of the identical electrodes, $r_s/a_0 = 3.01$ ²² for the Au contacts and is the ratio of the radius of the screening Fermi electron sphere to Bohr radius of the ground state

Hydrogen atom ($a_0 = 52.9$ pm). From (7), $r_{TF} = 58.8$ pm for the Au electrodes.

Figure 5 shows that electrochemical capacitance densities as high as $29 \text{ fF}/\mu\text{m}^2$ can be achieved using 1 nm thick SiO_2 despite reduced screening effects²¹. These are still high relative to currently attainable densities. At the above thickness, the difference between the electrostatic capacitance density of $35 \text{ fF}/\mu\text{m}^2$ and equivalent electrochemical capacitance density is 17%, which is quite significant. However this difference reduces as the dielectric thickness increases, and the electrochemical capacitance approaches the electrostatic capacitance.

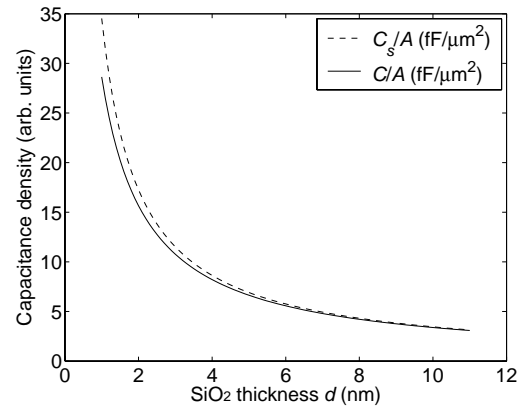


Figure 5. Capacitance density of SiO_2 nanocapacitor²¹ shown for electrostatic capacitance (broken line), and equivalent electrochemical capacitance resulting from reduced screening with $R = 1$ (solid line).

3.2 Operability at room temperature

When operated at room temperature, the I-V characteristics of nanocapacitors will differ dramatically between devices, owing to phononic and photonic scattering of stored electrons, especially given that they can only store tens or hundreds of electrons. This will pertain even if enclosed in shielded casing, as it is uneconomical to shield the nanocapacitors, and the nanocircuit they will operate in, from extraneous radiation. Even if extraneous radiation sources can be shielded, the electromagnetic energy from quantum vacuum fluctuations²³ will exert a limitation on the effectiveness of shielding, producing spontaneous excitation^{24, 25} of the stored electrons. Thus the nanoscale dimensions of the (polarized) dielectric imply large fluctuations in the I-V curves from small fluctuations in the quantity of electrons stored at any instant. Hence their I-V behavior depends on stochastics as well as on Fermi-Dirac statistics.

In addition, the fabrication mechanism if not well refined, will also have an impact on uniformity between devices. These non-uniformities can be minimized and their operability made possible at room temperature if the available states for charge carriers are quantum confined to low-dimensions (1D or 2D) such that charge

storage is monotonically dependent on the applied bias voltage, and the charges are less tolerant to extraneous excitations such as thermal and electromagnetic sources.

4. CONCLUSION

This work investigated the effects of material properties on the feasibility, and subsequent, operability of nanocapacitors, which are structures that are three dimensionally confined to nanoscale. In particular, this work demonstrated the effect of the dielectric, showing the result of the dielectric constant on the capacitance, and capacitance density, achieving $35 \text{ fF}/\mu\text{m}^2$ with the RPP nanocapacitor design. The importance of the dielectric strength to the maximum bias voltage the nanocapacitor can be charged to was also demonstrated, placing an upper limit on its charging capacity. Carefully engineering these structures electrically and physically may make possible SECs, which can find applications in single-electron memory devices.

Quantum electrical properties of the materials that may be used to implement nanocapacitors was also discussed, demonstrating the effect of reduced screening on spatially confined contacts due to the consequent low DOS. This resulted in an undesirable reduction of the capacitance density to $29 \text{ fF}/\mu\text{m}^2$ modeled by incorporating the Thomas-Fermi screening length of both metal contacts.

Capacitors are important circuit elements, and if nanocircuits are desirable in the future for higher efficiency, then nanocapacitors must also be developed in addition to nanoscale transistors. Nanocapacitors may find applications in low power, high-bandwidth, and real-time applications such as biochemically powered telemetry nanocircuits, and quantum charge pumps powering biomedical implants. They may also find uses in high fidelity, high-sensitivity proximity sensors, motion detectors, and actuators for nanoelectronic circuits and nanoelectromechanical systems (NEMS). These may range from capacitive and pressure-wave detectors to gravitational wave detectors used to detect illusive but predicted gravitational radiation.

REFERENCES

1. Semiconductor Industry Association, International Technology Roadmap for Semiconductors, 2002. Available: <http://public.itrs.net>.
2. Babcock, J.A., Balster, S.G., Pinto, A., Dirnecker, C., Steinmann, P., Jumper, R. and El-Kareh, B., Analog Characteristics of Metal-Insulator-Metal Capacitors Using PECVD Nitride Dielectrics, *IEEE Electron Device Letters* 2001, 22: 230-231.
3. Chen, S.B., Lai, C.H., Chin, A., Hsieh, J.C. and Liu, J., High-Density MIM Capacitors Using Al_2O_3 and AlTiO_x Dielectrics, *IEEE Electron Device Letters* 2002, 23: 185-187.
4. Ekanayake, S.R., Cortie, M.B. and Ford, M.J., Design of nanocapacitors and associated materials challenges, *Curr. Appl. Phys.* 4 (2-4): 250-254, 2004.
5. Kar-Roy, A., Hu, C., Racanelli, M., Compton, C. A., Kempf, P., Gurvinder, J., Sherman, P.N., Zheng, J., Zhang, Z. and Yin, A., High Density Metal Insulator Metal Capacitors Using PECVD Nitride for Mixed Signal and RF Circuits, *Proceedings of the IEEE International Interconnect Technology Conference* 1999, 1999: 245-247.
6. Macucci, M., Differential capacitance between circular stacked quantum dots, *Physica E* 1997, 1: 7-14.
7. Macucci, M., Hess, K. and Iafrate, G.J., Electronic energy spectrum and the concept of capacitance in quantum dots, *Physical Review B* 1993, 48: 17354-17363.
8. Wang, B., Zhao, X., Wang, J. and Guo, H., Nonlinear quantum capacitance, *Applied Physics Letters* 1999, 74: 2887-2889.
9. Wang, J., Guo, H., Mozos, J.L., Wan, C.C., Taraschi, G. and Zheng, Q., Capacitance of Atomic Junctions, *Physical Review Letters* 1998, 80: 4277-4280.
10. Mano, N., Mao, F. and Heller, A., Characteristics of a Miniature Compartment-less Glucose- O_2 Biofuel Cell and its Operation in a Living Plant, *Journal of American Chemical Society* 2003, 125: 6588-6594.
11. Mano, N., Mao, F. and Heller, A., A Miniature Biofuel Cell Operating in A Physiological Buffer, *Journal of American Chemical Society* 2002, 124: 12962-12963.
12. Dewan, C. and Teeters, D., Vanadia xerogel nanocathodes used in lithium microbatteries, *Journal of Power Sources* 2003, 119-121: 310-315.
13. Shnitov, V.V., Mikoushkin, V.M. and Gordeev, Y.S., Fullerite C_{60} as electron-beam resist for 'dry' nanolithography, *Microelectronic Engineering* 2003, 69: 429-434.
14. Prinz, V.Y., A new concept in fabricating building blocks for nanoelectronic and nanomechanic devices, *Microelectronic Engineering* 2003, 69: 466-475.
15. Aparicio, R. and Hajimiri, A., Capacity Limits and Matching Properties of Integrated Capacitors, *IEEE Journal of Solid-State Circuits* 2002, 37: 384-393.
16. Nakazato, K., Blaikie, R.J. and Ahmed, H., Single-electron memory, *Journal of Applied Physics* 1994, 75: 5123-5134.
17. Bersuker, G., Korkin, A., Fonseca, L., Safonov, A., Bagatur'yants, A. and Huff, H.R., The role of localized states in the degradation of thin gate oxides, *Microelectronic Engineering* 2003, 69: 118-129.
18. Chen, S. and Murray, R.W., Electrochemical Quantized Capacitance Charging of Surface Ensembles of Gold Nanoparticles, *Journal of Physical Chemistry B* 1999, 103: 9996-10000.
19. Zhou, C., Deshpande, M.R., Reed, M.A., Jones II, L. and Tour, J.M., Nanoscale metal/self-assembled monolayer/metal heterostructures, *Applied Physics Letters* 1997, 71: 611-613.
20. Black, C.T. and Welser, J.J., Electric-Field Penetration Into Metals: Consequences for High-Dielectric-Constant Capacitors, *IEEE Transactions on Electron Devices* 1999, 46: 776-780.

21. Ekanayake, S.R., Rodanski, B.S., Cortie, M.B. and Ford, M.J., Quantum Electrical Characteristics of Nanocapacitors, Third IEEE Conference on Nanotechnology 2003, 2: 756-759.
22. Ashcroft, N.W. and Mermin, N.D., Solid state physics, College ed, Saunders College Publishing, 1976.
23. Casimir, H.B.G., On the attraction between two perfectly conducting plates, Proceedings of the Koninklijke Nederlandse Akademie van Wetenschappen 1948, 51: 793.
24. Fujisawa, T., Oosterkamp, T.H., van der Wiel, W.G., Broer, B.W., Aguado, R., Tarucha, S. and Kouwenhoven, L.P., Spontaneous Emission Spectrum in Double Quantum Dot Devices, Science 1998, 282: 932-935.
25. Audretsch, J. and Müller, R., Spontaneous excitation of an accelerated atom: The contributions of vacuum fluctuations and radiation reaction, Physical Review A 1994, 50: 1755-1763.